0.5 for completely segregated streams and 0 for completely mixed streams. Figure 3D shows the evolution of σ for flows of different *Pe* in the SHM (open symbols), in a simple channel as in Fig. 3A (▲), and in a channel with straight ridges as in Fig. 3B (●). We see that the SHM performs well over a large range in *Pe*; as *Pe* increases by a factor of ~500 ($Pe = 2 \times 10^3$ to $Pe = 9 \times 10^5$), the mixing length, Δy_{90}, required for 90% mixing (dashed line), increases by less than a factor of 3 ($\Delta y_{90} = 0.7$ cm to $\Delta y_{90} = 1.7$ cm). In Fig. 3E, we see that Δy_{90} increases linearly with ln(*Pe*) for large *Pe*, as expected for chaotic flows. Within the limits of our simple model of mixing (*13*), we estimate from the linear portion of the plot in Fig. 3E that λ is on the order of a few millimeters; the average width of the filaments of unmixed fluid decreases by a factor of ~3 as the fluid travels this axial distance. This estimate agrees qualitatively with the evolution seen in Fig. 3C.

On the basis of the results presented in Fig. 3, consider mixing a stream of protein solution in aqueous buffer (molecular weight 10^5, $D \sim 10^{-6}$ cm^2/s) with $U = 1$ cm/s and $l = 0.01$ cm. For this system, $Pe = 10^4$. The mixing length in a simple microchannel would be $\Delta y_m \sim Pe \times l = 100$ cm. On the basis of Fig. 3D, the mixing length in the SHM would be, $\Delta y_m \sim 1$ cm. Furthermore, increasing the flow speed by a factor of 10 (i.e., to $Pe = 10^5$) will increase the mixing length in the SHM to $\Delta y_m \sim 1.5$ cm. With the same change in flow speed, the mixing length in the absence of stirring will increase 10-fold, to $\Delta y_m \sim 10^3$ cm.

An important application of mixing in pressure flows is in the reduction of axial dispersion. Axial dispersion is important in determining performance in pressure-driven chromatography—e.g., in the transfer of fractions from a separation column to a point detector—where it leads to peak broadening. The most rapid dispersion of a band of solute takes place when its axial length is much shorter than the mixing length of the solute in the flow. During this stage, the length of the band grows at the maximum speed of the flow (i.e., more quickly than the center of the band moves along the channel). This effect is illustrated schematically in the diagram in Fig. 4A for an unstirred Poiseuille flow. Once the length of the band is greater than the mixing length, volumes of fluid have sampled both fast and slow regions of the flow, and the broadening of the band becomes diffusive, i.e. $\sim \sqrt{D_{\mathrm{eff}}\tau_r}$, where D_{eff} is an effective diffusivity that again depends on the mixing length and τ_r is the residence time of the band in the flow (*8*, *25*).

The experiments presented in Fig. 4 demonstrate that, by stirring the fluid in the cross section of the flow, the SHM (Fig. 4C) reduces the extent of the initial, rapid broadening of a band of material relative to that in an unstirred flow (Fig. 4B). The mixing length in the unstirred flow is $\Delta y_m \sim 100$ cm. In this case, the asymmetry of the trace of fluorescence intensity as a function of time measured near the end of the channel (green trace in Fig. 4B) indicates that the band is still broadening rapidly as it reaches the end of the channel: The fluorescent fluid in the fast, uniform flow near the center of the channel is weakly dispersed and arrives at the detector first (steep initial rise of the trace); the fluorescent fluid in the shear flow near the walls is strongly dispersed and arrives at the detector later (long tail of the trace). With the SHM (Fig. 4C), the mixing length is $\Delta y_m \sim 1$ cm (estimated from the curves in Fig. 3D for $Pe = 10^4$). In this case, the band broadens rapidly in the first few centimeters of the channel as indicated by the asymmetry of the trace acquired 2 cm downstream from the inlet (blue trace in Fig. 4C). The traces acquired further downstream are noticeably more symmetrical; this change in-

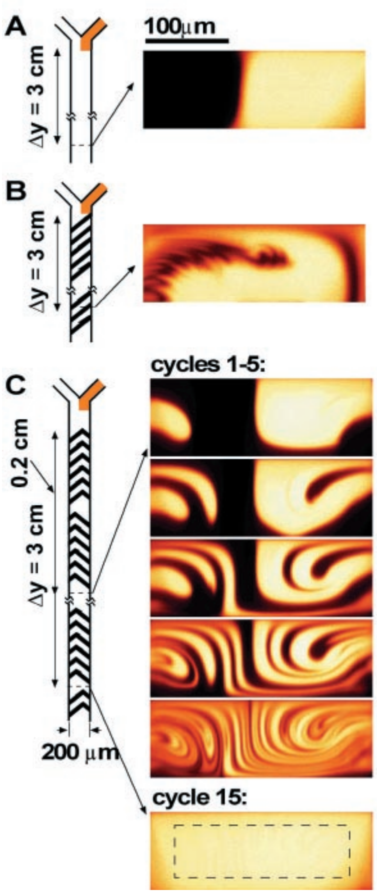

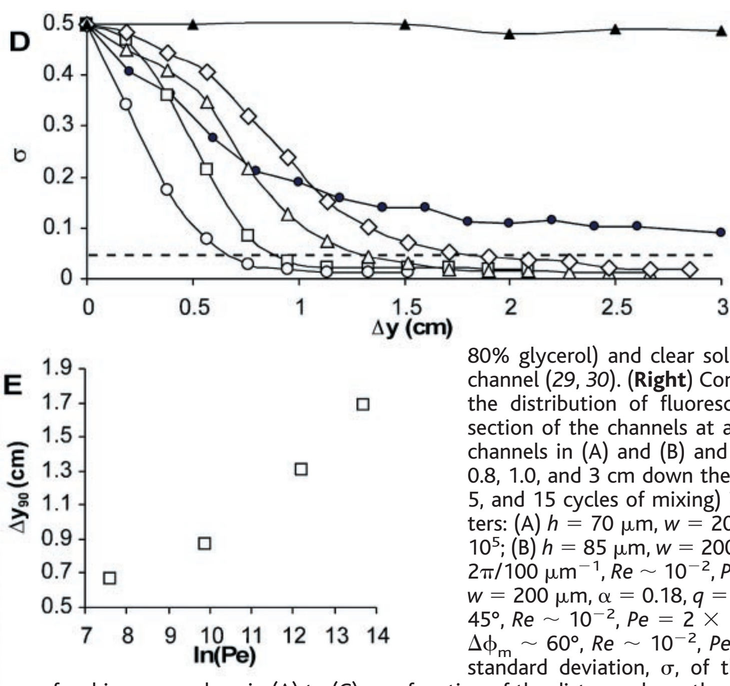

Fig. 3. Performance of SHM. (**A** to **C**) (**Left**) Schematic diagrams of channels with no structure on the walls (A), with straight ridges as in Fig. 1 (B), and with the staggered herringbone structure as in Fig. 2 (C). In each case, equal streams of a 1 mM solution of fluoroscein-labeled polymer in water/glycerol mixtures (0 and 80% glycerol) and clear solution were injected into the channel (*29*, *30*). (**Right**) Confocal micrographs that show the distribution of fluorescent molecules in the cross section of the channels at a distance of 3 cm down the channels in (A) and (B) and at distances of 0.2, 0.4, 0.6, 0.8, 1.0, and 3 cm down the channel (i.e., after 1, 2, 3, 4, 5, and 15 cycles of mixing) in (C). Experimental parameters: (A) $h = 70$ μm, $w = 200$ μm, $Re \sim 10^{-2}$, $Pe = 2 \times 10^5$; (B) $h = 85$ μm, $w = 200$ μm, $\alpha = 0.18$, $\theta = 45°$, $q = 2\pi/100$ μm^{-1}, $Re \sim 10^{-2}$, $Pe = 2 \times 10^5$; (C) $h = 85$ μm, $w = 200$ μm, $\alpha = 0.18$, $q = 2\pi/100$ μm^{-1}, $p = 2/3$, $\theta = 45°$, $Re \sim 10^{-2}$, $Pe = 2 \times 10^5$, six ridges per half-cycle, $\Delta\phi_m \sim 60°$, $Re \sim 10^{-2}$, $Pe = 9 \times 10^5$. (**D**) Plot of the standard deviation, σ, of the fluorescence intensity in confocal images such as in (A) to (C) as a function of the distance down the channel, Δ*y*. Only the central 50% of the area of the images [indicated in the bottom frame in (C)] was used to measure σ to eliminate variations in the fluorescence intensity due to optical effects at the channel walls. The open symbols are for the mixing channel in (C): (○) for $Pe = 2 \times 10^3$, (□) for $Pe = 2 \times 10^4$, (△) for $Pe = 2 \times 10^5$, and (◇) for $Pe = 9 \times 10^5$. $10^{-2} \le Re \le 10$ in these experiments. The points (▲) are for a smooth channel (A), and (●) are for a channel with straight ridges (B); for both, $Pe = 2 \times 10^5$. Horizontal dotted line indicates the value of σ used to evaluate Δy_{90}, the axial distance required for 90% mixing. (**E**) Plot of Δy_{90} as a function of ln(*Pe*) from the curves in (D).